Adsorption and thermal reactions of disilane and the growth of Si films on Ge(100)-(2×1)

D.-S. Lin, T. Miller, and T.-C. Chiang

Department of Physics, University of Illinois, 1110 West Green Street, Urbana, Illinois 61801
and Materials Research Laboratory, University of Illinois, 104 South Goodwin Avenue, Urbana, Illinois 61801

(Received 5 October 1992)

Scanning tunneling microscopy (STM), core-level photoemission spectroscopy using synchrotron radiation, and electron diffraction were employed to study the vapor-phase epitaxial growth of Si on Ge(100)-(2×1) using disilane (Si_2H_6). The dissociative chemisorption of a Si_2H_6 molecule on Ge(100)-(2×1) at room temperature results in two Si-trihydride (SiH_3) radicals bonded onto two adjacent Ge dangling bonds. Some SiH_2 and GeH species are also formed as a result of decomposition of SiH_3. An initial sticking coefficient of ~0.5 is deduced from STM images. An exposure of more than 2 langmuirs (1 langmuir$=10^{-6}$ Torr s) of disilane at room temperature saturates the surface with SiH_3, SiH_2, and GeH species, and the resulting surface is disordered. The total amount of Si on the saturated surface is about $\frac{1}{2}$ monolayer (ML). Successive annealing of the saturated surface to higher temperatures causes the conversion of SiH_3 to SiH_2, the conversion of SiH_2 to SiH, and the desorption of H from GeH. These processes become complete at about 600 K, and the resulting surface is a clean Ge(100)-(2×1) interspersed with about $\frac{1}{2}$ ML of Si-monohydride (SiH)-(2×1) islands. Desorption of hydrogen from these SiH islands occurs at even higher annealing temperatures, and is accompanied by indiffusion of Si into the Ge substrate. This process becomes complete at about 690 K, and the final system configuration is a clean Ge(100)-(2×1) with about $\frac{1}{2}$ ML of Si buried in the subsurface region. Multilayer Si deposition was performed by atomic layer epitaxy, i.e., cyclic disilane adsorption at ~340 K followed by thermal conversion at 820 K. For up to 18 cycles, the resulting surface consists of Ge only. The change in surface morphology is studied by STM. Differences between the clean Si(100)-(2×1) and Ge(100)-(2×1) surfaces as observed by STM are also reported.

I. INTRODUCTION

Among various epitaxial growth processes, vapor-phase epitaxy (VPE) is the most important for silicon devices.[1] The surface chemical reactions and growth mechanisms involved in this process have been a subject of much technological and scientific interest. Four Si vapor-phase sources, including silicon tetrachloride ($SiCl_4$), trichlorosilane ($SiHCl_3$), dichlorosilane (SiH_2Cl_2), and silane (SiH_4) have been widely used in the past. The typical substrate temperature for Si growth using these gases ranges from about 1170 K (for SiH_4) to 1470 K (for $SiCl_4$).[1] To achieve a lower growth temperature, an effort has been made to find alternate chemical vapor sources, and disilane (Si_2H_6) has been demonstrated to be an excellent choice.[2–4] Compared with silane, disilane has a much higher adsorption coefficient due to a lower decomposition activation energy for the Si-Si bond in Si_2H_6 than that for the Si-H bond in SiH_4; consequently, epitaxial films can be grown at a much lower substrate temperature.

The adsorption and growth of disilane on Si(100)-(2×1) has been studied extensively using a number of techniques including infrared spectroscopy,[5] thermal desorption,[5] secondary-ion mass spectrometry,[6] scanning tunneling microscopy,[7,8] electron-energy-loss spectroscopy,[9] electron diffraction,[9] and photoemission spectroscopy.[10] it is known that disilane adsorbs molecularly at low temperatures (below 90 K).[2] As the substrate temperature is raised, the adsorbed disilane molecules decompose, leading to the sequential formation of trihydride (SiH_3), dihydride (SiH_2), and monohydride (SiH) radicals, and the final desorption of all hydrogen from the surface. The conversions from one hydride to the next do not necessarily occur at sharply defined annealing temperatures. At 130 K, it is observed that SiH_3 is the dominant species. At room temperature, all three hydride species show significant populations.[5] The conversion to SiH from the higher hydrides does not become complete until an annealing temperature of ~620 K is reached. Upon annealing to ~770 K, all remaining hydrogen atoms desorb from the surface and about $\frac{1}{2}$ monolayer (ML) epitaxial Si film is left on the surface. This low temperature and self-limiting growth mechanism has been demonstrated to be practical for a layerwise, or "atomic-layer-epitaxy," growth process.[3]

The present work is a study of the VPE growth of Si on Ge(100). Heteroepitaxy of Si and Ge on each other is of interest in both fundamental science and optoelectronic device applications.[11] Because Si and Ge have very similar properties, it is expected that Si VPE growth on Ge should be generally similar to that for Si on Si. However, previous growth studies based on the solid-phase molecular-beam-epitaxy (MBE) technique show interesting differences between the Si-on-Ge and Ge-on-Si systems. For Ge on Si(100), the growth is epitaxial and layer by layer for the first 2–3 atomic layers followed by three-dimensional island growth at temperatures up to

 ©1993 The American Physical Society

~670 K without any noticeable intermixing,[12–14] while the growth of Si on Ge(100) in the same temperature range is characterizted by Si indiffusion and intermixing.[15,16] This indiffusion is observed even at room temperature, and can be attributed at least partially to the lower surface free energy of Ge. The present work provides an interesting comparison between Si VPE growth on Ge(100) and the corresponding MBE process.

The techniques employed in this study include core-level photoemission spectroscopy using synchrotron radiation, scanning tunneling microscopy, and electron diffraction. This system has also been examined in a separate study by electron-energy-loss and electron-diffraction techniques.[17] The complementary nature of these techniques allows us to collect detailed information. The results indicate that Si VPE growth on Ge(100) using disilane is indeed similar to the corresponding growth on Si(100), but not identical. The relevant reactions are summarized as follows:

$$Si_2H_6 \rightarrow 2SiH_3(s) , \quad (1)$$

$$SiH_3(s)+Ge(s) \rightarrow SiH_2(s)+GeH(s) , \quad (2)$$

$$GeH(s) \rightarrow Ge(s)+\tfrac{1}{2}H_2(g) , \quad (3)$$

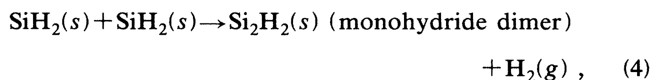

$$SiH_2(s)+SiH_2(s) \rightarrow Si_2H_2(s) \text{ (monohydride dimer)} + H_2(g) , \quad (4)$$

and

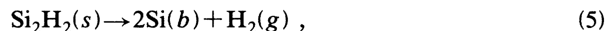

$$Si_2H_2(s) \rightarrow 2Si(b)+H_2(g) , \quad (5)$$

where (s), (b), and (g) indicate a surface species, an atom in the substrate below the surface, and a desorbed gas molecule, respectively. Equations (1), (2), and (4) are fairly similar to those for Si VPE growth on Si(100). Equation (5) exhibits the major difference; here, hydrogen desorption from Si monohydride is accompanied by Si indiffusion into the Ge substrate. This indiffusion is similar to that observed in the MBE growth of Si on Ge,[16] except that it does not occur until the substrate temperature is high enough for hydrogen desorption from Si. The decomposition of disilane into SiH_3, SiH_2, and SiH is also similar to that for disilane on Ge(111) as studied recently by infrared spectroscopy.[18]

We have examined multilayer growth following the standard procedure for atomic-layer epitaxy. The Ge surface is first saturated with disilane at near room temperature, and then annealed to high temperatures to desorb the hydrogen. This results in a net deposition of about $\frac{1}{2}$ ML of Si atoms, which diffuse into the subsurface region. This quantized deposition process is repeated. We show that, for up to 18 cycles, the resulting surface consists of Ge only. STM pictures reveal the roughening of the surface during this growth process.

II. EXPERIMENTAL DETAILS

The scanning tunneling microscope used in this study has been described in a previous publication.[19] All of our results to be presented below were obtained with a sample bias of -2 V and a tunneling current of 0.3 nA. The photoemission measurements were performed at the Synchrotron Radiation Center of the University of Wisconsin–Madison. A large hemispherical analyzer was used to collect and analyze the photoelectrons. The photocurrent from a gold mesh positioned in the synchrotron beam path was monitored for a relative measurement of the incident photon beam flux.

The Ge(100) samples, of size $0.35\times1.2\times0.04$ cm^3, were cut from commercial n-type wafers with a resistivity of about 1 Ω cm. Cyclic sputtering with 500-eV Ar^+ followed by heating to ~1100 K for about 20 s yielded a clean surface exhibiting a sharp (2×1) diffraction pattern. Disilane was introduced into the chamber through a precision leak valve. To avoid exciting the disilane molecules, the ionization gauge in the vacuum chamber was turned off during the exposure. The dosing pressure, in the range of 10^{-8}–10^{-7} Torr, was monitored by the ion-pump current, which was calibrated before the experiment using the ionization gauge. The pressure reading was corrected for the ionization gauge sensitivity of disilane, which is 2.4 relative to air.[4] Successive annealing of the disilane-saturated sample was performed by resistive heating of the sample itself, and each anneal lasted 60 s. The temperature of the sample as a function of heating power was calibrated by attaching a very small thermocouple to the center of the front face of an identical test sample. The estimated accuracy of the temperature measurement is about ±20 K.

III. ROOM-TEMPERATURE ADSORPTION AND THERMAL ANNEALING

A. Electron-diffraction patterns

The starting Ge(100) surface shows a sharp (2×1) pattern. Exposing the surface to increasing amounts of disilane at room temperature causes the background to increase and the half-order spots to weaken relative to the primary spots. The pattern does not change any more after the exposure exceeds about 2 langmuirs (L), indicating that the surface has been saturated. The higher background suggests that the surface is partially disordered. The half-order spots are still clearly visible after saturation, implying that a significant number of Ge dimer bonds on the surface remain intact. In contrast, the closely related Si(100)-(2×1) surface saturated by disilane shows a (1×1) pattern with a high background, implying that most, if not all, dimer bonds on the surface are broken.[9] As we will discuss below, breakage of the dimer bond on the surface is associated with the decomposition of SiH_3 to form SiH_2 [see Eq. (2)]. Our electron-diffraction observation is consistent with a recent report.[17]

B. Core-level photoemission results

Figure 1, taken from Ref. 16, shows surface-sensitive Si $2p$ and Ge $3d$ core-level spectra for clean Si(100)-(2×1) and Ge(100)-(2×1), respectively, and the results of a least-squares analysis. Each spectrum is analyzed in terms of three spin-orbit-split components S, S', and B of identical line shape, which correspond to signals derived

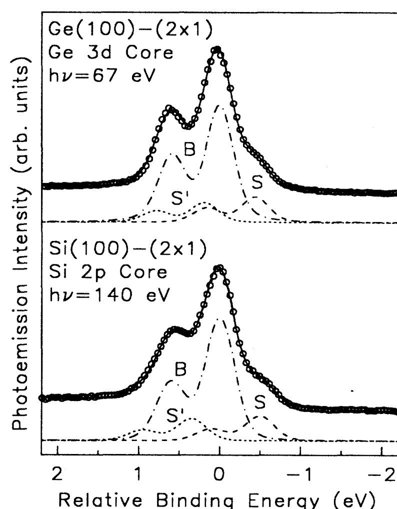

FIG. 1. Photoemission spectra (circles) for the Si $2p$ and Ge $3d$ core levels of Si(100)-(2×1) and Ge(100)-(2×1), respectively. The photon energies used are indicated. The solid curves are fits to the spectra. The curves labeled *S*, *S*′, and *B* are the results of a decomposition of the spectra into contributions from the top layer, the second layer, and the bulk, respectively.

from the dimerized surface layer, the second layer, and the bulk, respectively. The *S* component is responsible for the shoulder on the lower binding-energy side. The relatively weak *S*′ component is not visually resolved from the *B* component due to the small energy shift, but its existence has been confirmed in a number of studies.[12,20–22] The effect of the *S*′ component can be satisfactorily simulated by a slight increase of the width and a very slight shift of the *B* component to include the contribution of the *S*′ component. The present study will adopt this approximation; namely, the spectra will be fitted with just two components (*B* and *S*). This poses no problem, since the focus here is on the *S* component, which is the main signature of the clean (2×1) reconstruction. Our two-component fit might not yield accurate intensities, but since all spectra are fitted the same way, the systematic trend in the intensity changes deduced from the fit should be quite reliable.

We need to mention that there exist other interpretations of these core-level spectra. Although the *S* component is undoubtedly derived from the dimer layer, there are different opinions concerning the atomic population corresponding to its emission intensity. In the above interpretation, the *S* component is attributed to one full monolayer of atoms on the surface, including both the up and down dimer atoms. In some other interpretations,[20,22] the *S* component is attributed to the up dimer atoms only (one-half of a monolayer). We will refer to these different interpretations as the full-layer and half-layer interpretations, respectively. Our data have been analyzed both ways, and the conclusions are the same. To save space, we will mainly adopt the full-layer interpretation in the wording of the qualitative discussion. The minor changes necessary for the other interpretation are obvious. The quantitative analysis of the core-level intensity to be presented below is carried out in a way independent of the choice of the interpretation.

Figure 2 shows Si $2p$ core-level spectra for various exposures of disilane on Ge(100)-(2×1) at room temperature. The binding-energy scale is referred to the bulk component of the Ge $3d_{5/2}$ line. Using this energy reference, the effect of band bending induced by changing surface conditions is removed. All of the other Ge and Si core-level results to be presented below use the same energy reference. Figure 2 shows that the Si $2p$ photoemission intensity increases monotonically and saturates after a total exposure of ~2 L. The line shape remains essentially the same for all exposures up to 50 L, suggesting that the relative abundances of various surface Si species are nearly independent of the exposure. The broadness of the line shape can be attributed to disorder, the presence of different hydride species on the surface, and possibly vibrational excitations of Si-H bonds that are observed in the spectra of gas-phase silane and disilane.[23]

Figures 3(a) and 3(b) show the Si $2p$ and Ge $3d$ core-level spectra, respectively, for successive anneals to higher temperatures after saturating the Ge(100) surface with a 10-L disilane exposure at 310 K. Again, the binding-energy scale is referred to the bulk component of the Ge $3d_{5/2}$ line. After saturation exposure, the *S* component of the Ge $3d$ disappears. As the annealing temperature increases, the *S* component begins to reappear around 530 K. With a two-component fit as described above, the intensity ratio of the *S* and *B* components, I_S/I_B, is plotted in Fig. 4(a). After annealing to beyond 690 K, this ratio saturates at about 0.21, which is just slightly higher than the value of 0.20 for the clean Ge(100)-(2×1) surface. The broadness of the Si $2p$ spectra, shown in Fig. 3(a), and the lack of distinct features

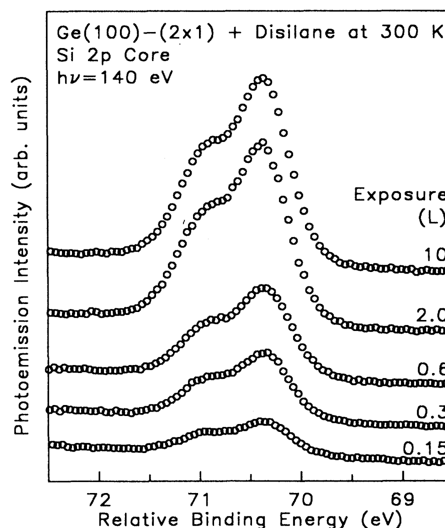

FIG. 2. Photoemission spectra of Si $2p$ for various disilane exposures on Ge(100)-(2×1) at 300 K. The binding-energy scale is referred to the Ge $3d_{5/2}$ bulk component. The photoemission intensity of each spectrum has been normalized to the incident photon beam intensity.

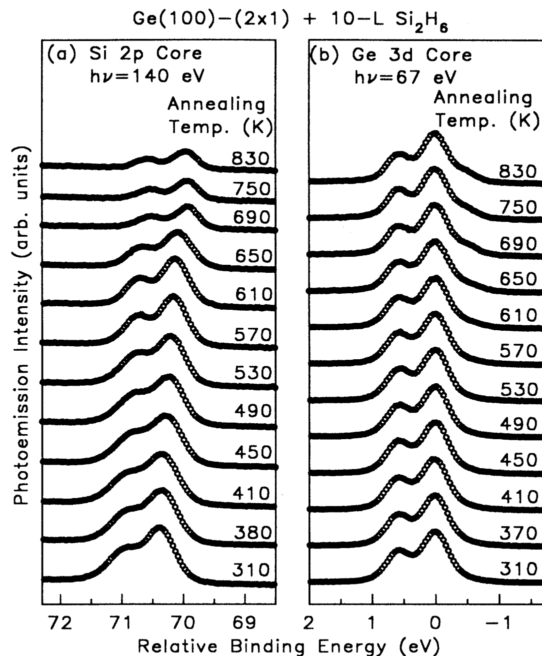

FIG. 3. Photoemission spectra for (a) Si $2p$ and (b) Ge $3d$ core levels for various annealing temperatures as indicated. The sample is Ge(100) initially saturated by a 10-L disilane exposure at room temperature. The relative binding-energy scales are referred to the Ge $3d_{5/2}$ bulk component. The photoemission intensity of each spectrum has been normalized to the incident photon beam intensity.

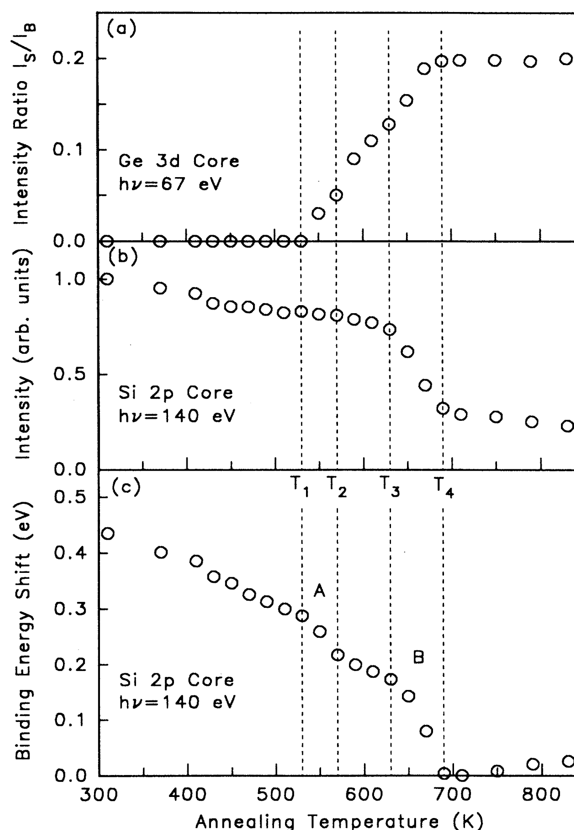

FIG. 4. (a) Intensity ratio (I_S/I_B) of the S and B components of Ge $3d$, (b) integrated intensity of Si $2p$, and (c) binding-energy shift of Si $2p$ as a function of annealing temperature. The sample is Ge(100) initially saturated by a 10-L disilane exposure at room temperature. Two temperature ranges A and B and four temperatures T_1-T_4 are indicated.

for individual components make a detailed analysis in terms of individual components impossible. It can be seen that the line shape changes, shifts, and diminishes in intensity for increasing annealing temperatures. We employed a single-component fit, with a variable width, to find the total integrated intensity and the relative average binding energy; these are plotted in Figs. 4(b) and 4(c), respectively. In Fig. 4(c), we can identify two temperature ranges, indicated by A and B in the figure, in which the curve shows significantly steeper slopes. This kind of behavior suggests certain transitions or reactions. The relevant temperatures defining these two ranges are the following: $T_1=530$ K, $T_2=570$ K, $T_3=630$ K, and $T_4=690$ K, which are also correlated with various break or onset points in the other curves in Fig. 4.

C. STM results and model development

1. Room-temperature adsorption

Since the Si-Si bond in disilane is the easiest to cleave,[24] it is natural to expect that the dissociative chemisorption of disilane of Ge(100) will involve two SiH_3 radicals as indicated by Eq. (1). The SiH_3 radicals are highly reactive; once generated, they will react with nearby dangling bonds immediately. An important consequence is that two nearby dangling bonds on the Ge(100)-(2×1) surface will be saturated by a single disilane molecule. Figure 5 shows various adsorption geometries. The clean Ge(100)-(2×1) surface has a dimerized structure, and each surface atom has a dangling bond. In adsorption configuration A, two SiH_3 fragments bond onto adjacent dangling bonds of two dimers in the same dimer row separated by 4.0 Å. Configuration B involves two dan-

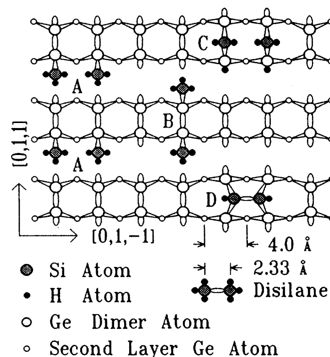

FIG. 5. Schematic diagrams for various bonding configurations of disilane fragments on Ge(100)-(2×1).

gling bonds of the same dimer, separated by about 2.4 Å. The Si-Si bond length in disilane is 2.33 Å.[24] Based on geometry alone, one would expect configuration B to be more favorable than configuration A, but this is opposite to our experimental observation to be described below.

The adsorbed SiH_3 radical may decompose to form a SiH_2 by releasing a hydrogen atom to a nearby Ge dangling bond as shown in configuration C in Fig. 5 [see Eq. (2)]. Note that in this process, one Ge dimer bond is broken for each SiH_2 formed on the surface, and the substrate geometry changes from (2×1) to (1×1) locally. For disilane adsorption on Si(100)-(2×1), it is known that most SiH_3 radicals are converted to SiH_2 at room temperature, and indeed the resulting saturated surface shows a (1×1) diffraction pattern. As stated above, the Ge(100) case is different in that the (2×1) half-order spots are still quite visible after saturation adsorption of disilane at room temperature, indicating that many dimer bonds remain intact. Thus, we expect to see a significant SiH_3 population on this surface.

In all of our scanning tunneling microscopy (STM) images presented below, a low spatial frequency filtering is applied to enhance the local contrast. The images resemble landscapes with light illumination from the western sky. The pictures are somewhat distorted by thermal drift. Figures 6(a) and 6(b) show 210×250 Å^2 STM images for Ge(100)-(2×1) exposed to 0.02 and 0.3 L of disilane at room temperature, respectively. In these images, both symmetric and asymmetric Ge dimers are seen, in agreement with precious reports.[25] The bright bumps can be identified as the reacted sites, which become more numerous as the exposure increases. These reacted sites are stable at room temperature, and show no preference for step edges. The majority (about three quarters) of the reacted sites involve two neighboring dimers in the same dimer row, and the bumps are biased to one side of the dimer row. This is consistent with the adsorption geometry A shown in Fig. 5. There are also reacted sites characterized by bright bumps on the two dangling bonds of the same dimer, which are consistent with configuration B. In addition, one finds sites involving two neighboring dimers in the same dimer row, and the bright bumps appear centered about the dimer row. We believe that these correspond to configuration C. Figure 6(b) shows that at higher coverages, the reacted sites in configuration A tend to form chains; the local relationship is schematically indicated by the two neighboring A sites shown in Fig. 5, both biased in the same direction. Thus, adsorption on one site renders the adjacent sites on neighboring dimer rows more favorable for adsorption. Apparently, each neighboring dimer pair on a dimer row can accommodate only one disilane molecule. The remaining dangling bonds become inaccessible for further adsorption; this can be either an electronic effect or a geometric blocking effect. The ideal coverage at saturation based on configuration A should be 0.5 ML of Si. From a counting of the number of reacted sites in Fig. 6(b) and the known exposure of 0.3 L, we deduce an initial sticking coefficient of about 0.5. In other words, every disilane molecule striking the surface has a 50% chance of sticking to the surface.

As the disilane coverage increases, antiphase defects in the arrangement of the A sites and the presence of other bonding configurations result in disorder. Figure 7(a) shows an image over an area of 500×500 Å^2 of Ge(100)-(2×1) saturated with 5-L disilane at room temperature. Three monatomic steps across the area at about 45° angle can be discerned. The reacted sites do not show any long-range order, although there are some short chains.

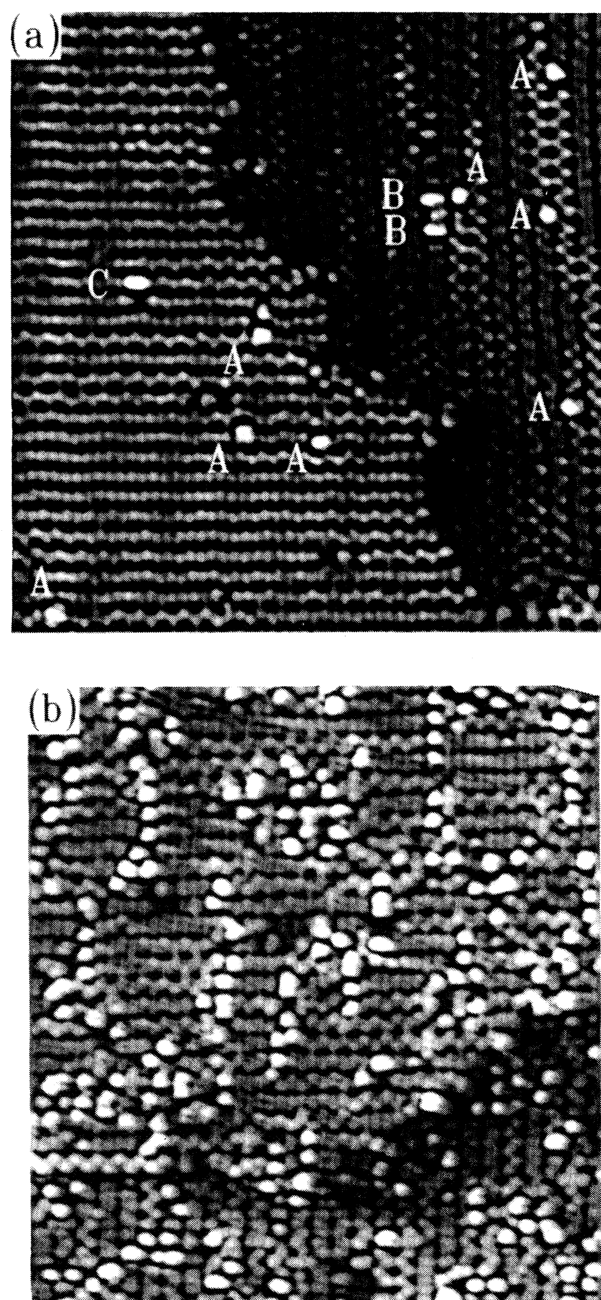

FIG. 6. STM images of Ge(100)-(2×1) dosed by (a) 0.02 L and (b) 0.3 L of disilane at room temperature. The areas are 210×250 Å^2.

2. *Transition A*

Figures 7(b) and 7(c) show 500×500 Å^2 STM pictures after annealing to 530 and 620 K, respectively, for the room-temperature saturated surface. These temperatures are just before the two transition regions *A* and *B*, respectively, marked in Fig. 4. Between room temperature and T_1, the surface remains disordered. Figure 7(b), taken after annealing to T_1, shows a disordered surface, with some chainlike structures. Figure 7(c) is taken after transition *A*, but before transition *B*. Here, one sees a Ge(100)-(2×1) surface interspersed with well-ordered (2×1) islands covering about 40–50 % of the surface (nominally $\frac{1}{2}$ ML). Thus, transition *A* in Fig. 4 is associated with diffusion and coalescence of Si species on the surface to form ordered (2×1) islands. Because SiH_2 exhibits a locally (1×1) structure, the (2×1) reconstruction indicates that the islands are either SiH or pure Si (see Fig. 5). The latter possibility can be ruled out, since pure Si is not stable on Ge (it will indiffuse) at these annealing temperatures.[16] This is very similar to the case of disilane on Si(100)-(2×1) previously studied,[8] in which (2×1) Si-monohydride islands are formed after annealing to similar temperatures.

The onset of transition *A* at T_1 is marked by a rise of the intensity of the *S* component of the Ge 3*d* core level,

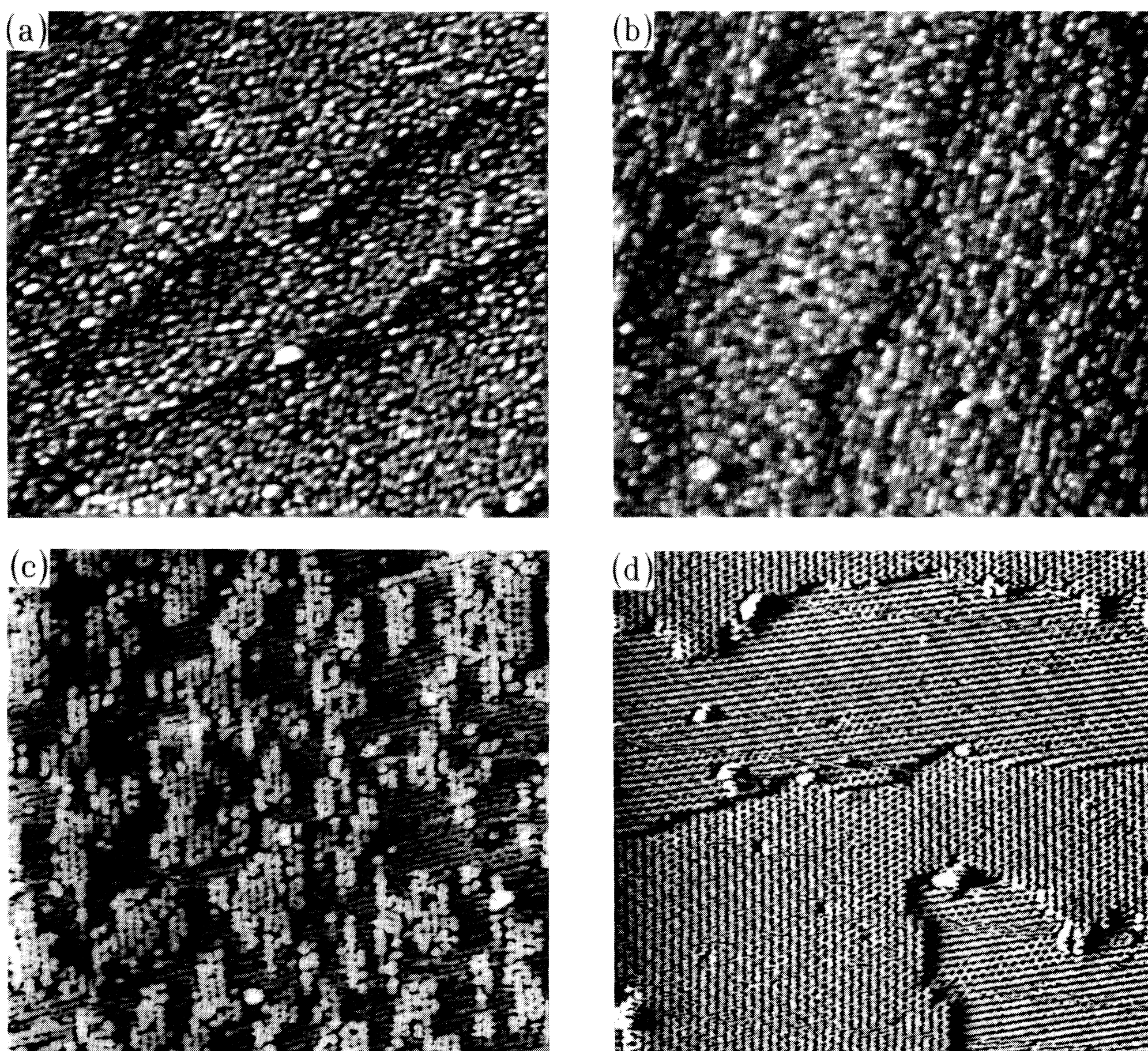

FIG. 7. STM images of (a) Ge(100)-(2×1) saturated with a 5-L disilane dose at 300 K and the same surface after annealing to (b) 530 K, (c) 620 K, and (d) 720 K. The scanned areas are 500×500 Å^2.

as shown in Fig. 4(a). The intensity of the S component is a measure of the surface area that is clean Ge(100)-(2×1) (it does not matter whether we use the full- or half-layer interpretation). Thus, the diffusion and coalescence of Si-hydride species on the surface is accompanied by the partial exposure of the clean Ge(100)-(2×1) surface. The data in Fig. 4(a) show that the surface after annealing to 620 K exhibits an I_S/I_B ratio about $\frac{1}{2}$ of that of the clean Ge(100)-(2×1) surface. Therefore, about $\frac{1}{2}$ of the sample surface must be clean Ge(100)-(2×1), and this is consistent with the STM picture shown in Fig. 7(c).

According to Eq. (2), the formation of $\frac{1}{2}$ ML SiH_2 on the surface is accompanied by the formation of $\frac{1}{2}$ ML of Ge monohydride (GeH). Upon annealing through transition A, the SiH_2 radicals combine to form $\frac{1}{2}$-ML SiH islands as discussed above. Since the core-level results indicate that the exposed Ge surface is clean, the $\frac{1}{2}$-ML H on GeH must have desorbed from the Ge surface as indicated by Eq. (3). This is consistent with previous thermal desorption studies, which show that significant desorption of H from GeH begins at about 500–550 K, while SiH persists to much higher temperatures.[26,27]

Based on the data in Fig. 4(b), the amount of Si on the surface remains relatively constant within 20% between room temperature and the onset of transition B. Since the island coverage at the onset of transition B is about 40–50 % of the surface, the initial Si coverage at room temperature is about 0.5–0.6 ML (nominally $\frac{1}{2}$ ML). The 20% reduction of the Si intensity before transition B could be due to desorption of Si in the form of SiH_4. It is also possible that a small amount of Si diffuses into the substrate.

3. *Transition B*

Transition B in Fig. 4 is marked by a rapid decrease of the average Si $2p$ binding energy and a large reduction of the Si $2p$ intensity. After this transition, the Ge $3d$ I_S/I_B ratio becomes essentially the same as that of clean Ge(100)-(2×1). These observations indicate that the clean Ge(100)-(2×1) surface has been restored, the $\frac{1}{2}$-ML Si must have diffused into the subsurface region, and all of the hydrogen atoms have been desorbed. This indiffusion of Si is very similar to that observed for Si MBE growth on Ge(100),[16] and is related to the observation of Ge segregation induced by thermal annealing of Si-Ge alloys.[27] In MBE growth, the indiffusion of Si is observed even at room temperature. For the present system, the hydrogen atoms on the Si-monohydride island apparently hinder the indiffusion, and thus indiffusion occurs only after hydrogen desorption. From previous studies,[4–9] hydrogen desorption from SiH on Si(100) is negligible at $T_4=690$ K, the end of transition B, yet our surface is already without hydrogen at this temperature. This implies that the desorption of H from the SiH islands on Ge is aided by some other mechanisms. One possible scenario is that the desorption of H is enhanced by the free-energy gain from Si indiffusion, and the desorption and indiffusion together constitute a single step with a lower barrier. This mechanism will require the concerted atomic motions of Si, Ge, and H. A more likely explanation is that the hydrogen atoms on SiH become mobile and diffuse off the island edge, where they can be desorbed from the Ge surface. Previous laser spectroscopy studies of H diffusion on Si indicates that this is a good possibility.[28]

Figure 7(d) shows a STM picture taken after annealing to 720 K, a temperature beyond transition B. Here one observes Ge dimer rows in four terraces separated by three atomic steps. The middle step is of type A, and the other two are of type B. In this particular picture, no islands are seen, although other pictures do show the presence of large islands which have not been incorporated into terraces (see below).

Note that transition B is accompanied by a change in the Si $2p$ core-level binding energy by about 0.18 eV. This can be attributed to a chemical shift induced by bonding to a hydrogen atom.[29] In other words, replacing a Si-Si or Si-Ge bond by a Si-H bond leads to a binding-energy increase of the Si by 0.18 eV.

We now perform a simple intensity analysis of the Si and Ge core levels across transition B using the standard layer attenuation model. This model states that the emission intensity is reduced by a factor of $\exp(-d/l)$ for each atomic layer on top of the emitter. Here, $d=1.4$ Å is the interlayer spacing for Ge(100), and l is the phenomenological escape depth. Figure 4 shows a reduction of the Si $2p$ intensity to 30% across the transition. Assuming that all of the Si atoms after the transition settle in the second layer, we would have $\exp(-d/l)=0.3$ and $l=1.2$ Å. This value of l is much too small.[29] In order to account for the large reduction of the Si $2p$ intensity, we have to allow in our model that a significant number of Si atoms move into deeper layers in the Ge substrate; that is, a Si-Ge alloy is formed in the subsurface region. This conclusion is independent of the question whether we use the full- or half-layer interpretation. The presence of $\frac{1}{2}$ ML of Si in the subsurface region will cause the emission intensity of the B component of Ge $3d$ to decrease. An analysis based on either interpretation shows that I_S/I_B of Ge $3d$ should become slightly larger than the clean value, which is in agreement with our observation. Unfortunately, our data are insufficient for a determination of the layer-resolved Si concentration profile in the subsurface region. It is quite possible that the Si concentration as a function of depth below the surface shows a gradient as well as oscillations.[30] Within the half-layer interpretation, it is also possible that some Si atoms occupy the positions of down dimer atoms after the transition, but the number of these atoms must be quite small.

4. *Annealing behavior between room temperature and transition A*

Having explained transitions A and B, we now examine the annealing behavior between room temperature and T_1, in which the changes of the system are more gradual. The main change is in the average Si $2p$ core-level binding energy shown in Fig. 4(c), which can be understood in terms of the chemical shifts associated with mul-

tiple ligands. Previous studies have established a "multiple-ligand rule"; namely, the chemical shift induced by N ligands is approximately N times the chemical shift induced by a single ligand.[29] Since SiH shows a chemical shift of 0.18 eV as noted above, SiH_2 and SiH_3 must show chemical shifts of about 0.36 and 0.54 eV, respectively. In Fig. 4(c), the gradual reduction of the average Si 2p chemical shift from about 0.44 eV at room temperature to about 0.29 eV at T_1 is consistent with an initial mixture of SiH_3 and SiH_2 which gradually decomposes to form a mixture of SiH_2 and SiH. The decomposition is gradual probably because the surface species are largely immobile and the reactions do require either an available neighboring site [Eq. (2)] or the combination of two surface radicals that must be adjacent to each other [Eq. (4)]. This immobility is implied by the STM observation that up to T_1 there is no long-range order and no island formation [see Fig. 7(b)]. T_1 is therefore likely the onset of significant long-range diffusion of surface species, allowing the conversion of all remaining SiH_2 to form SiH islands.[8]

The Si 2p core-level line shape shown in Fig. 3 remains quite broad until the annealing temperature exceeds about 570 K (the best way to judge the broadness is to look at the relative depth of the valley between the two spin-orbit peaks). This is consistent with the notion that before transition A, the system is a mixture of different hydrides with different, unresolved chemical shifts.

IV. MULTILAYER GROWTH BY ATOMIC-LAYER EPITAXY

As noted above, saturating the Ge(100) surface with disilane at room temperature followed by high-temperature annealing yields a net deposition of about $\frac{1}{2}$-ML of Si. Repeating this cycle results in a controlled, quantized deposition generally known as atomic-layer epitaxy. In our study, we chose an initial saturation exposure of 5 L and an annealing temperature of 820 K. This annealing temperature represents a compromise. Higher temperatures will promote step flow and island incorporation for a smoother growth, but the indiffusion of Si and intermixing between Si and Ge will also be enhanced. If a fairly abrupt interface is desired, one should try to use as low a growth temperature as possible. Figure 4(b) shows that the Si 2p intensity continues to decline for increasing annealing temperatures beyond transition B, which is a sign of continued indiffusion. As noted above, the $\frac{1}{2}$-ML Si deposited in the first cycle forms a Si-Ge alloy in the subsurface region. This intermixing process is expected to continue as the deposition cycle is repeated at 820 K. The choice of this particular growth temperature is motivated by our previous work on the homoepitaxial growth of Si on Si(100) using Si_2H_6; we found the growth to be smooth (layer by layer) via the mechanism of step flow at this temperature.

Figures 8(a) and 8(b) show representative photoemission spectra of Si 2p and Ge 3d after various numbers of cycles of Si deposition. The intensity of Si 2p increases monotonically for increasing Si depositions, but the line shape remains fairly sharp and unchanged. There is no

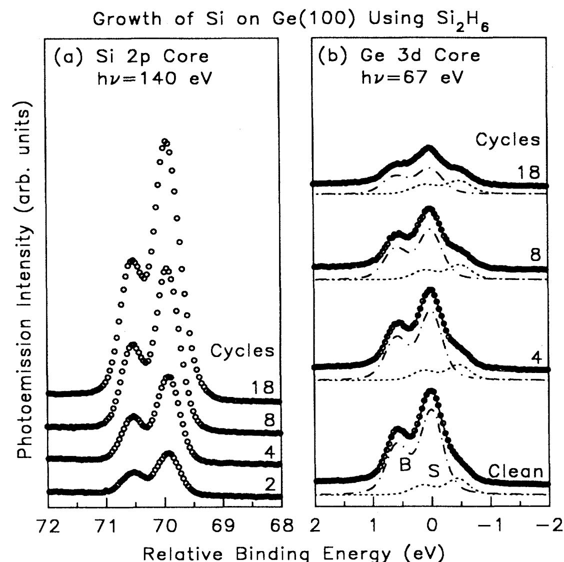

FIG. 8. Photoemission spectra (circles) of (a) Si 2p and (b) Ge 3d for various numbers of cycles of Si growth on Ge(100). Each cycle involves an exposure of 5-L disilane at 340 K followed by annealing at 820 K. The curves in (b) show the overall fits (solid curves) and the decomposition into the S and B components.

sign of the S component (see Fig. 1) for up to 18 cycles, implying that all of the Si atoms have moved below the surface. The Ge 3d spectra have been analyzed using the two-component fit mentioned above, and the results are shown by the various curves in the figure. Even without the fit, it is clear from a visual inspection that the emission from the S component remains approximately unchanged while the emission from the B component diminishes as more Si is deposited. The intensities of the Ge S and B components from the fit are shown in Fig. 9. The fairly constant Ge S intensity indicates that the composi-

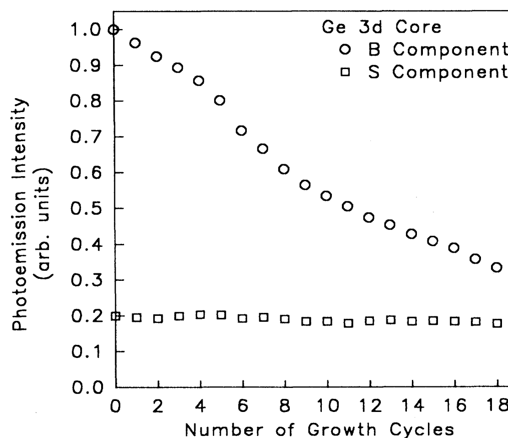

FIG. 9. Photoemission intensities for the B and S components of Ge 3d for various numbers of cycles of Si growth on Ge(100). Each cycle involves an exposure of 5-L disilane at 340 K followed by annealing at 820 K.

tion of the top atomic layer remains nearly 100% Ge. After 18 cycles of Si deposition, the Ge B intensity decays to 33% of the clean surface value. This intensity is larger than what one would expect if all of the deposited Si forms a pure Si slab under the Ge dimer layer. Our result can be explained by the formation of a Si-Ge alloy layer in the subsurface region. It is likely that the alloy concentration is not spatially uniform, but we cannot determine this variation from our data. The interpretation of the intensity is also complicated by the fact that the surface roughens as the growth proceeds (see below). A recent study of the MBE growth of Si on Ge(100) at similar temperatures, based on the Z-contrast transmission electron microscopy technique, clearly reveals the intermixing of Si and Ge.[31]

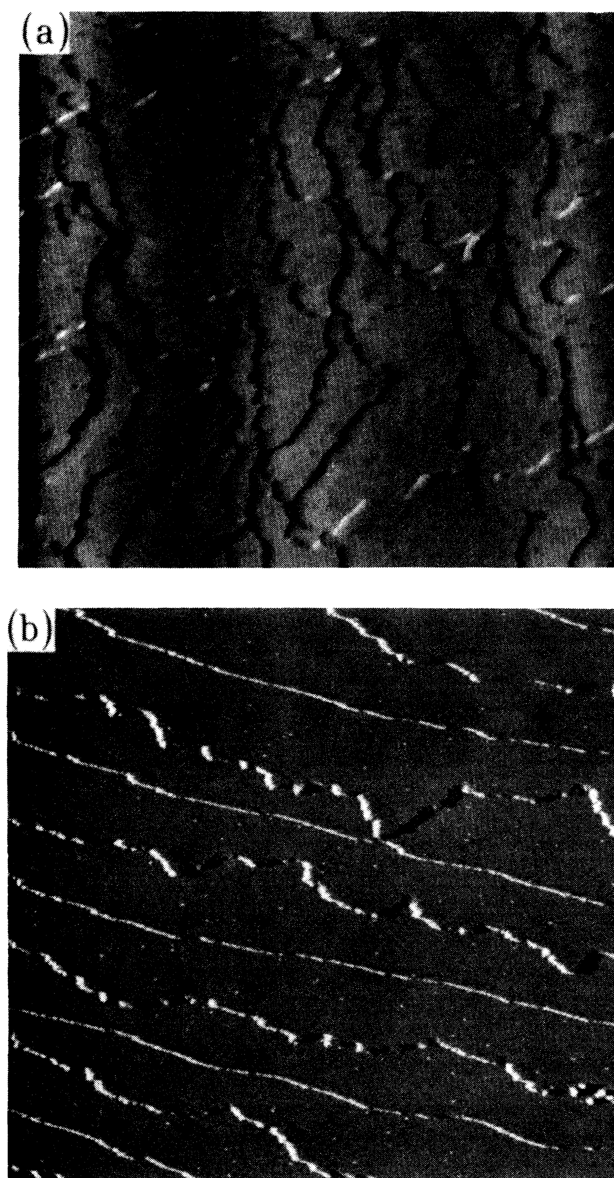

FIG. 10. STM images (4000×4000 Å^2) of (a) Ge(100)-(2×1) and (b) Si(100)-(2×1).

Figure 10(a) shows a 4000×4000 Å^2 STM image of our clean Ge(100)-(2×1) after sputtering and annealing to 1100 K. Individual atoms and dimers cannot be seen at this scale, and the linelike features are atomic steps. From the step density, a miscut angle of 0.2°–0.3° is deduced. For comparison, Fig. 10(b) shows an image of Si(100)-(2×1) surface with about the same miscut angle, prepared by flash heating to $\sim$1400 K in the usual manner. This image confirms the earlier findings about the Si(100) step structure: the steps are alternately smooth and rough, which correspond to the so-called type A and B steps, respectively. The average spacings between neighboring steps are approximately constant. This behavior has been explained in terms of the minimization of the long-range strain field extending into the bulk Si substrate.[32] In contrast, the step structure of Ge(100)-(2×1) is quite random, and the steps do not show the alternately smooth and rough appearance. This observed difference is not likely due to the different annealing temperatures, because in our preparation of the samples, the annealing temperature of the Ge surface (1100 K) is closer to the Ge bulk melting point (1210 K) than the flash temperature of Si (1400 K) to the Si bulk melting point (1680 K). It appears, therefore, that the detailed energetics of strain interaction and/or step formation for Ge(100)-(2×1) is different from that for Si(100)-(2×1).

We have observed another interesting difference between Si and Ge. There is typically a few percent of dimer defects on Si(100) as reported by many workers.[33] The Ge(100) surface, on the other hand, shows few defects [for example, see Fig. 6(a)].

Figure 11 shows a sequence of 4000×4000 Å^2 images. Figures 11(a) and 11(b) show disilane-saturated Ge(100)-(2×1) surface after annealing to 720 and 820 K, respectively. At these annealing temperatures, the hydrogen atoms are desorbed and the Si atoms have moved below the surface. Many large Ge islands on terraces are observed in Fig. 11(a). The effect of raising the annealing temperature is to cause these Ge islands to be incorporated into neighboring terraces by step flow, as seen in Fig. 11(b). During this process, all Si atoms must remain buried below the surface. The atomic movement of Si during Ge island formation and step flow is an interesting issue,[31,34] but it cannot be addressed in detail here. We will not offer any speculative model. Figure 11(b) shows that some very large islands remain on the surface after an 820-K anneal; otherwise the surface appears very much like the clean surface.

Repeating the cycle of saturation adsorption followed by annealing to 820 K results in increased surface roughness. Figures 11(c) and 11(d) show the surface after 5 and 10 cycles of growth, respectively. This roughening, or reduction of the terrace sizes, is incompatible with the assumption that the incorporation of islands into terraces occurs on a fixed length scale comparable to the average terrace width as seen in Fig. 11(b). Probable causes for the roughening include the strain associated with the 4% lattice mismatch between Se and Ge and the effect of Ge

segregation to the surface. This interpretation is supported by the fact that deposition of Si on Si(100) using disilane at the same temperature results in smooth growth,[8] for which mismatch and segregation do not play a role. Even though the surface shown in Fig. 11(d) is rough, the local structure remains (2×1). Figure 12 is a 500×500 Å^2 image of the surface after 10 cycles of growth. The dimer structure is seen on all terraces. However, the density of defects within each terrace, in the form of "missing dimers," has significantly increased. Again, this might be due to the mismatch strain and/or the effect of Ge segregation. Similar defects have been reported in the MBE growth of Ge on Si(100), which have been attributed to the Ge-Si mismatch.[35,36]

V. SUMMARY

By combining information from spectroscopic, microscopic, and diffraction studies, we have obtained a good understanding of the adsorption and thermal reactions of disilane on Ge(100) and the resulting growth of Si. This is one of the simplest systems of heteroepitaxial VPE growth. In this study, we have made a number of interesting observations: (1) The dissociative chemisorp-

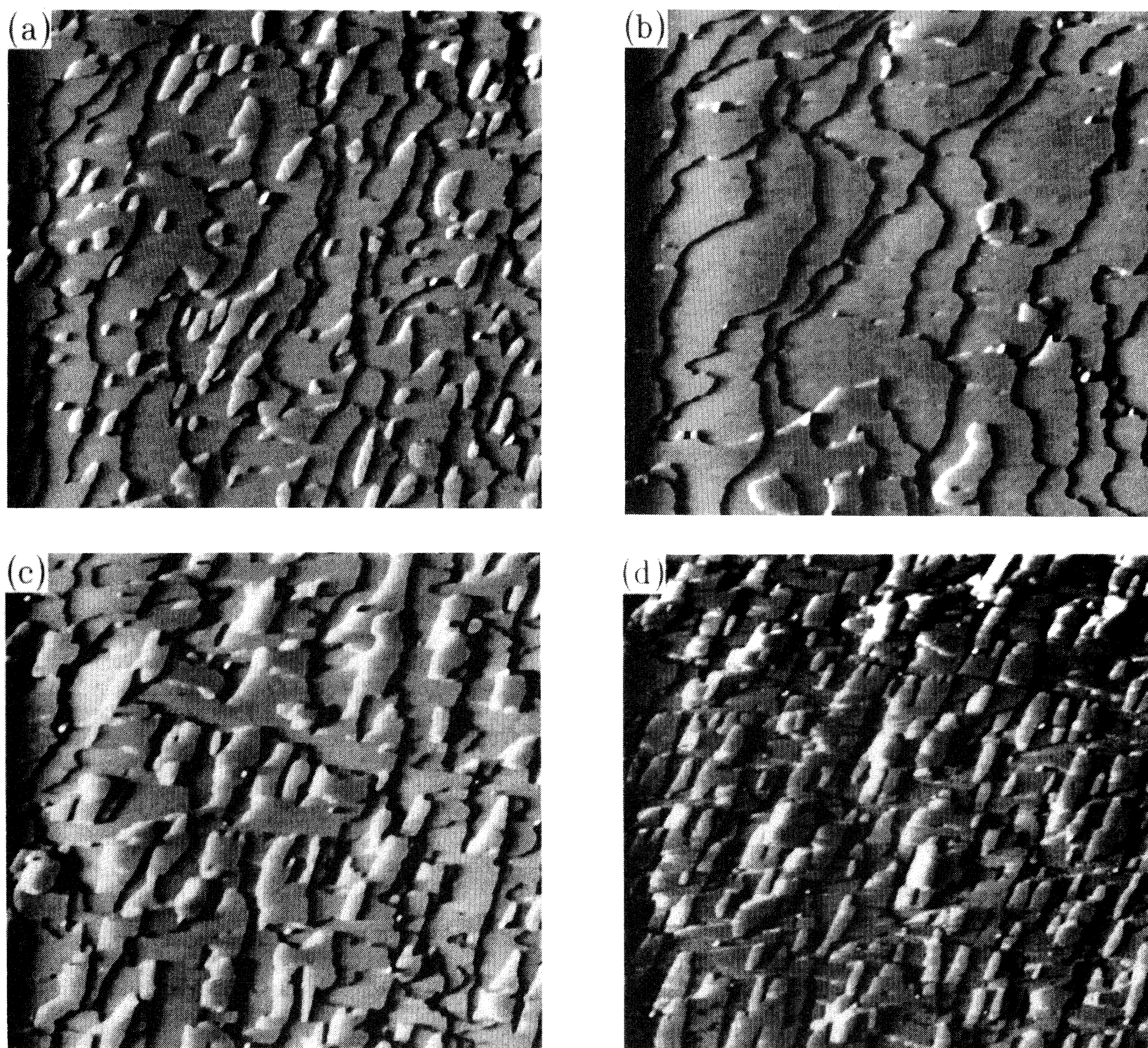

FIG. 11. (a) and (b) show 4000×4000 Å^2 STM images of Ge(100)-(2×1), exposed to 5-L disilane at room temperature and then annealed to 720 and 820 K, respectively. (c) and (d) show the same scale images of Ge(100)-(2×1) after (c) 5 and (d) 10 cycles of Si growth. Each cycle involves an exposure of 5-L disilane at 340 K followed by annealing at 820 K.

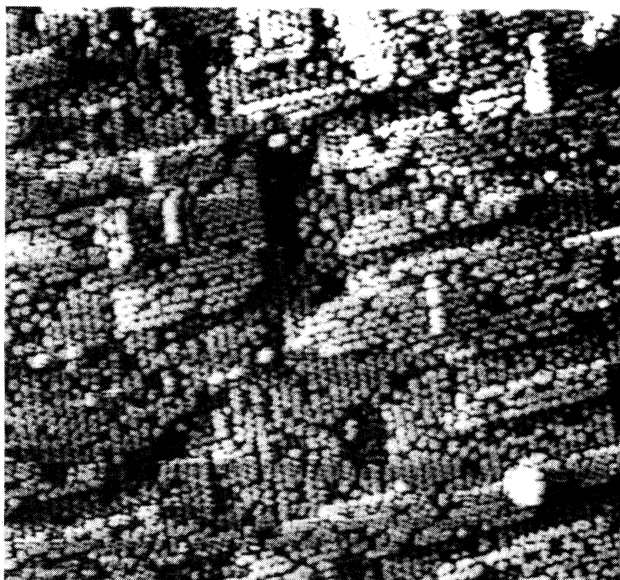

FIG. 12. A 500×500 Å^2 STM image of Ge(100) after 10 cycles of Si growth. Each cycle involves an exposure of 5-L disilane at 340 K followed by annealing at 820 K.

tion of a Si_2H_6 molecule involves two neighboring dangling bonds on the surface. (2) The sticking coefficient can be deduced by counting reacted sites in STM pictures. (3) The conversion of SiH_3 to SiH_2 during progressive annealing is a fairly gradual process, probably because of the lack of long-range diffusion of surface species. (4) The Si atoms tend to move below the surface, but the H on SiH hinders this movement. (5) The desorption temperature of H from SiH islands on Ge(100) is significantly lower than that of H from the Si(100) surface. (6) Annealing the disilane-saturated surface to high temperatures results in a net deposition of about $\frac{1}{2}$ ML of Si in the subsurface region; the composition of the surface atomic layer remains nearly 100% Ge. (7) The coarsening of islands and the incorporation of islands into terraces must be accompanied by Si moving into the subsurface region after H desorption. Exactly how this works on an atomic level remains an interesting question. (8) Multilayer growth by atomic-layer epitaxy at 820 K results in a surface that is relatively rough and shows a significant number of defects. Strain due to mismatch and Ge segregation are probable causes. (9) There are interesting differences in the step structure and defect density between the clean Si(100)-(2×1) and Ge(100)-(2×1) surfaces.

ACKNOWLEDGMENTS

The authors wish to thank R. Tsu and J. E. Greene for assistance. This material is based upon work supported by the U.S. Department of Energy (Division of Materials Science, Office of Basic Energy Sciences), under Grant No. DEFG02-91ER45439. Acknowledgment is also made to the Donors of the Petroleum Research Fund, administered by the American Chemical Society, and to the U.S. National Science Foundation (Grant No. DMR-89-19056) for partial personnel and/or equipment support. We acknowledge the use of central facilities of the Materials Research Laboratory of the University of Illinois, which is supported by the U.S. Department of Energy (Division of Materials Science, Office of Basic Energy Sciences), under Grant No. DEFG02-91ER45439, and the U.S. National Science Foundation under Grant No. DMR-89-20538. The Synchrotron Radiation Center of the University of Wisconsin–Madison is a national user facility supported by the U.S. National Science Foundation.

[1]S. M. Sze, *Semiconductor Devices, Physics and Technology* (Wiley, New York, 1985).
[2]F. Bozso and Ph. Avouris, Phys. Rev. B **38**, 3943 (1988).
[3]D. Lubben, R. Tsu, T. R. Bramblett, and J. E. Greene, J. Vac. Sci. Technol. A **9**, 3003 (1991); H. Hirayama, T. Tatsumi, and N. Aizaki, Appl. Phys. Lett. **52**, 1484 (1988).
[4]S. M. Gates, Surf. Sci. **195**, 307 (1988); R. Imbihl, J. E. Demuth, S. M. Gates, and B. A. Scott, Phys. Rev. B **39**, 5222 (1989).
[5]G. Lu, Ph.D. thesis, University of California at San Diego, 1992 (unpublished).
[6]S. M. Gates and C. M. Chiang, Chem. Phys. Lett. **184**, 448 (1991).
[7]J. J. Boland, Phys. Rev. B **44**, 1383 (1991).
[8]D.-S. Lin, E. S. Hirshorn, T.-C. Chiang, R. Tsu, D. Lubben, and J. Greene, Phys. Rev. B **45**, 3494 (1992).
[9]Y. Suda, D. Lubben, T. Motooka, and J. E. Greene, J. Vac. Sci. Technol. A **8**, 61 (1990).
[10]D.-S. Lin, T. Miller, and T.-C. Chiang (unpublished).
[11]See, for example, Thin Solid Films **183** (1989).
[12]D.-S. Lin, T. Miller, and T.-C. Chiang, Phys. Rev. Lett. **67**, 2187 (1991); J. E. Rowe and G. K. Wertheim, *ibid.* **69**, 550 (1992); F. J. Himpsel, *ibid.* **69**, 551 (1992); D.-S. Lin, J. A. Carlisle, T. Miller, and T.-C. Chiang, *ibid.* **69**, 552 (1992).
[13]J. Tersoff, Phys. Rev. B **43**, 9377 (1991); Y. Kataoka, H. Ueba, and C. Tatsuyama, J. Appl. Phys. **63**, 749 (1988).
[14]Y.-W. Mo, D. E. Savage, B. S. Swartzentruber, and M. G. Lagally, Phys. Rev. Lett. **65**, 1020 (1990).
[15]A. J. Hoeven, J. Aarts, and P. K. Larsen, J. Vac. Sci. Technol. A **7**, 5 (1989).
[16]D.-S. Lin, T. Miller, and T.-C. Chiang, Phys. Rev. B **45**, 11 415 (1992).
[17]R. Tsu, D. Lubben, T. R. Bramblett, J. E. Greene, D.-S. Lin, and T.-C. Chiang, Surf. Sci. (to be published).
[18]J. E. Crowell and G. Lu, J. Electron. Spectrosc. Relat. Phenom. **54/55**, 1045 (1990).
[19]F. M. Leibsle, A. Samsavar, and T.-C. Chiang, Phys. Rev. B **38**, 5780 (1988).
[20]G. K. Wertheim, D. M. Riffe, J. E. Rowe, and P. H. Citrin, Phys. Rev. Lett. **67**, 120 (1991).
[21]X. Yang, R. Cao, J. Terry, and P. Pianetta, Phys. Rev. B **45**, 13 749 (1992).

[22]E. Landemark, C. J. Karlsson, Y.-C. Chao, and R. I. G. Uhrberg, Phys. Rev. Lett. **69**, 1588 (1992).

[23]J. D. Bozek, G. M. Bancroft, J. N. Cutler, and K. H. Tan, Phys. Rev. Lett. **65**, 2757 (1990); Z. F. Liu, G. M. Bancroft, J. N. Cutler, D. G. Sutherland, K. H. Tan, J. S. Tse, and R. G. Cavell, Phys. Rev. A **46**, 1688 (1992).

[24]P. M. Agrawal, D. L. Thompson, and L. M. Raff, J. Chem. Phys. **92**, 1069 (1990).

[25]J. A. Kubby, J. E. Griffith, R. S. Becker, and J. S. Vickers, Phys. Rev. B **36**, 6079 (1987).

[26]L. Surnev, and M. Tikhov, Surf. Sci. **138**, 40 (1984).

[27]J. A. Schaefer, J. Q. Broughton, J. C. Bean, and H. H. Farrell, Phys. Rev. B **33**, 2999 (1986); H. H. Farrell, J. Q. Broughton, J. A. Schaefer, and J. C. Bean, J. Vac. Sci. Technol. A **4**, 123 (1986).

[28]G. A. Reider, J. Hofer, and T. F. Heinz, Phys. Rev. Lett. **66**, 1994 (1991).

[29]F. J. Himpsel, F. R. McFeely, J. F. Morar, A. Taleb-Ibrahimi, and J. A. Yarmoff, in *Photoemission and Adsorption Spectroscopy of Solids and Interfaces with Synchrotron Radiation*, Proceedings of the International School of Physics "Enrico Fermi," Course CVIII, Varenna, 1988, edited by G. Scoles (North-Holland, New York, 1990); T.-C. Chiang, CRC Crit. Rev. Solid State Mater. Sci. **14**, 269 (1988).

[30]P. C. Kelires and J. Tersoff, Phys. Rev. Lett. **63**, 1164 (1989).

[31]D. E. Jesson, S. J. Pennycook, and J.-M. Baribeau, Phys. Rev. Lett. **66**, 750 (1991).

[32]O. L. Alerhand, D. Vanderbilt, R. D. Meade, and J. D. Joannopoulos, Phys. Rev. Lett. **61**, 1973 (1987).

[33]R. A. Wolkow, Phys. Rev. Lett. **68**, 2636 (1992), and references therein.

[34]R. M. Tromp, A. W. Denier van der Gon, and M. C. Reuter, Phys. Rev. Lett. **68**, 2313 (1992).

[35]Y. W. Mo and M. G. Lagally, J. Cryst. Growth **111**, 876 (1991); U. Kohler, O. Jusko, B. Muller, M. Horn-von Hoegen, and M. Pook, Ultramicrosc. **42-44**, 832 (1992).

[36]J. Tersoff, Phys. Rev. B **45**, 8833 (1992).

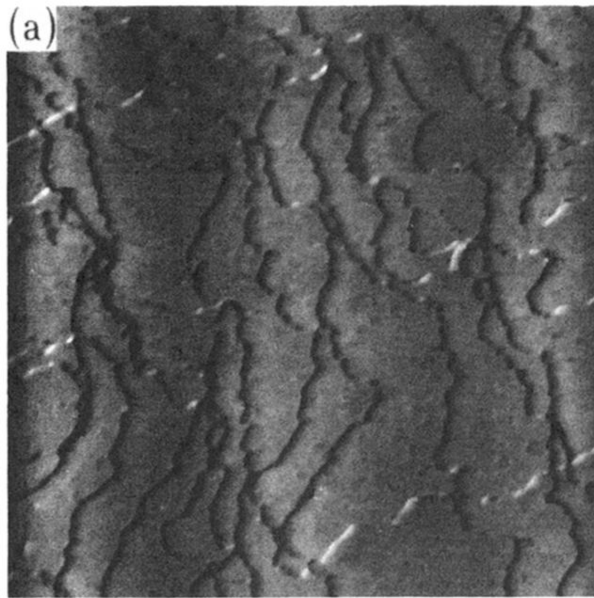

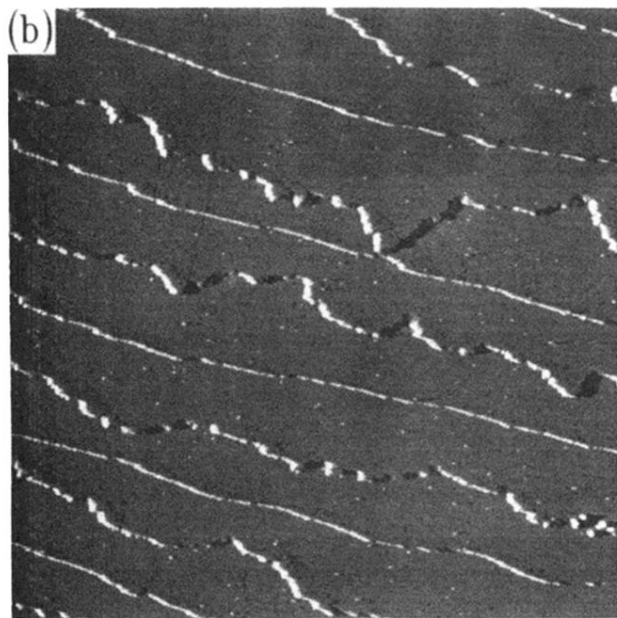

FIG. 10. STM images (4000×4000 Å^2) of (a) Ge(100)-(2×1) and (b) Si(100)-(2×1).

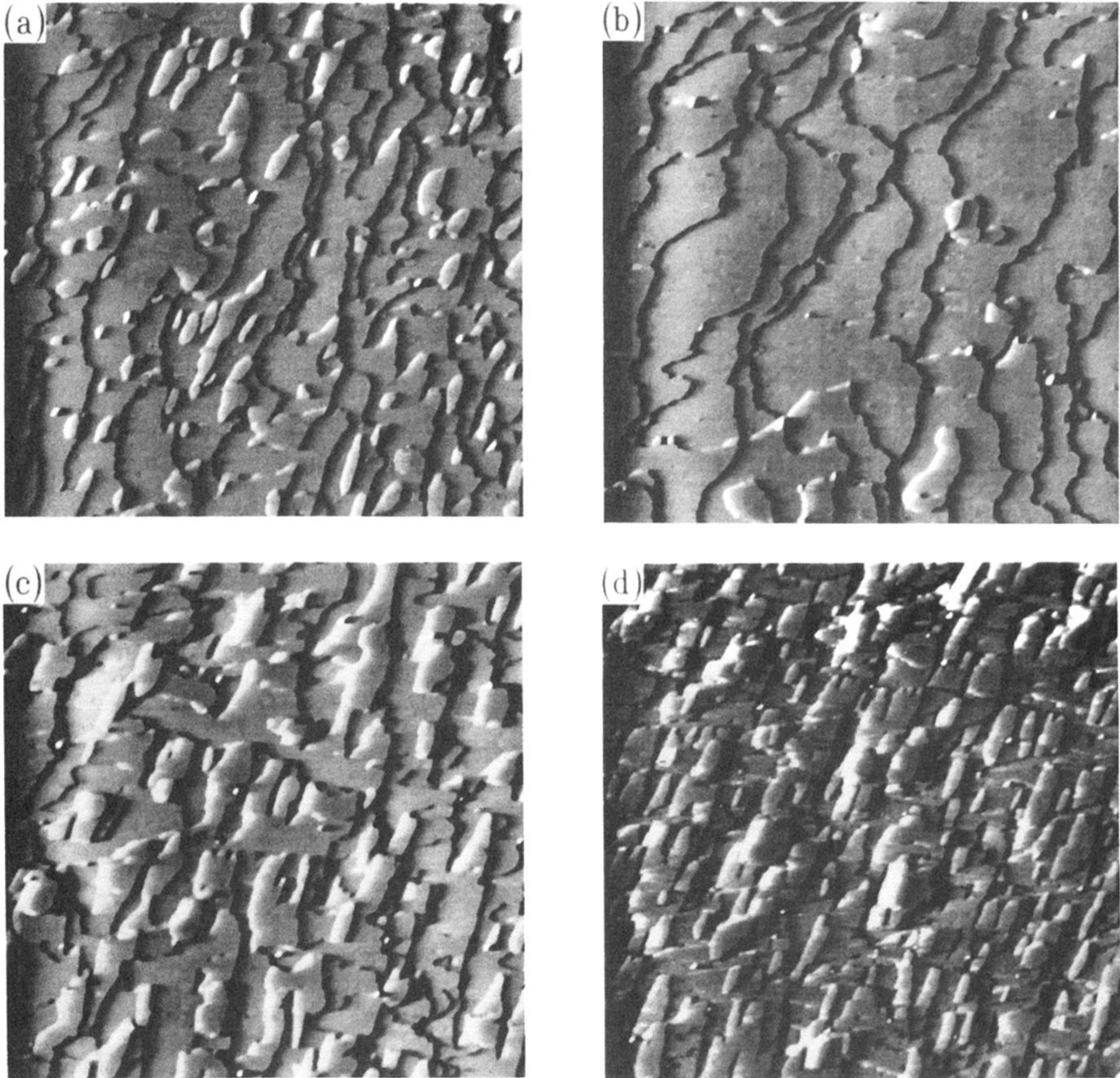

FIG. 11. (a) and (b) show 4000×4000 Å^2 STM images of Ge(100)-(2×1), exposed to 5-L disilane at room temperature and then annealed to 720 and 820 K, respectively. (c) and (d) show the same scale images of Ge(100)-(2×1) after (c) 5 and (d) 10 cycles of Si growth. Each cycle involves an exposure of 5-L disilane at 340 K followed by annealing at 820 K.

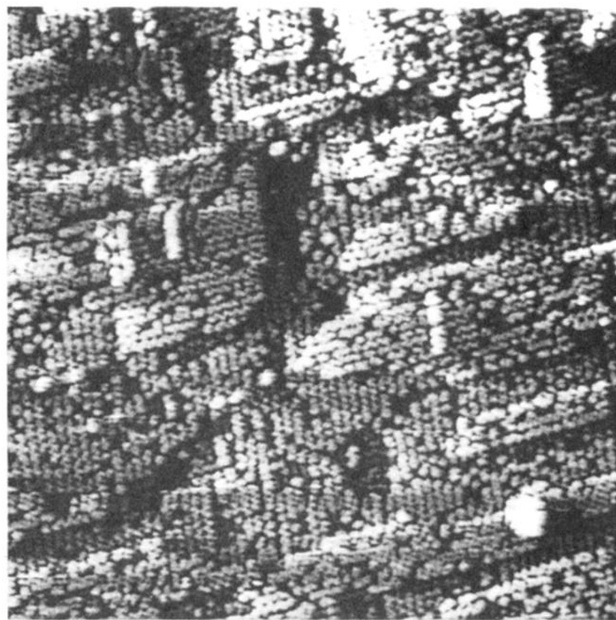

FIG. 12. A 500×500 Å^2 STM image of Ge(100) after 10 cycles of Si growth. Each cycle involves an exposure of 5-L disilane at 340 K followed by annealing at 820 K.

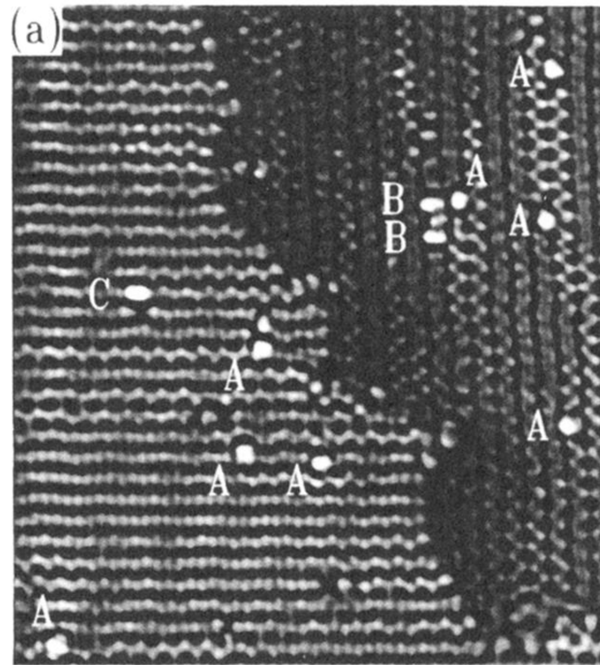

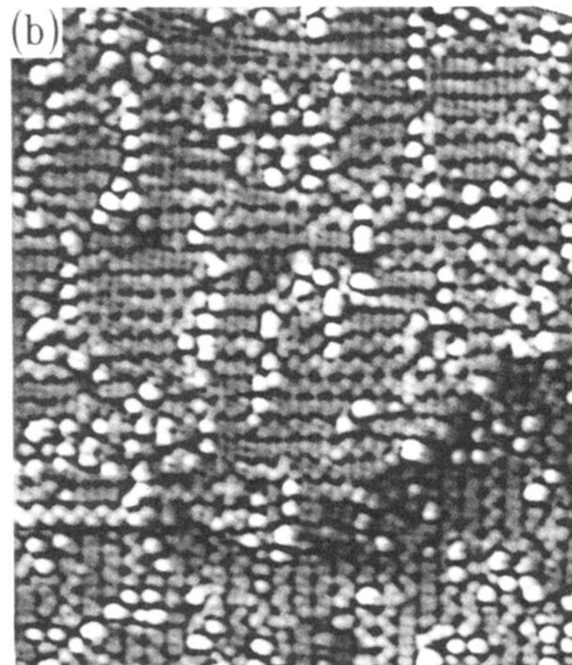

FIG. 6. STM images of Ge(100)-(2×1) dosed by (a) 0.02 L and (b) 0.3 L of disilane at room temperature. The areas are 210×250 $Å^2$.

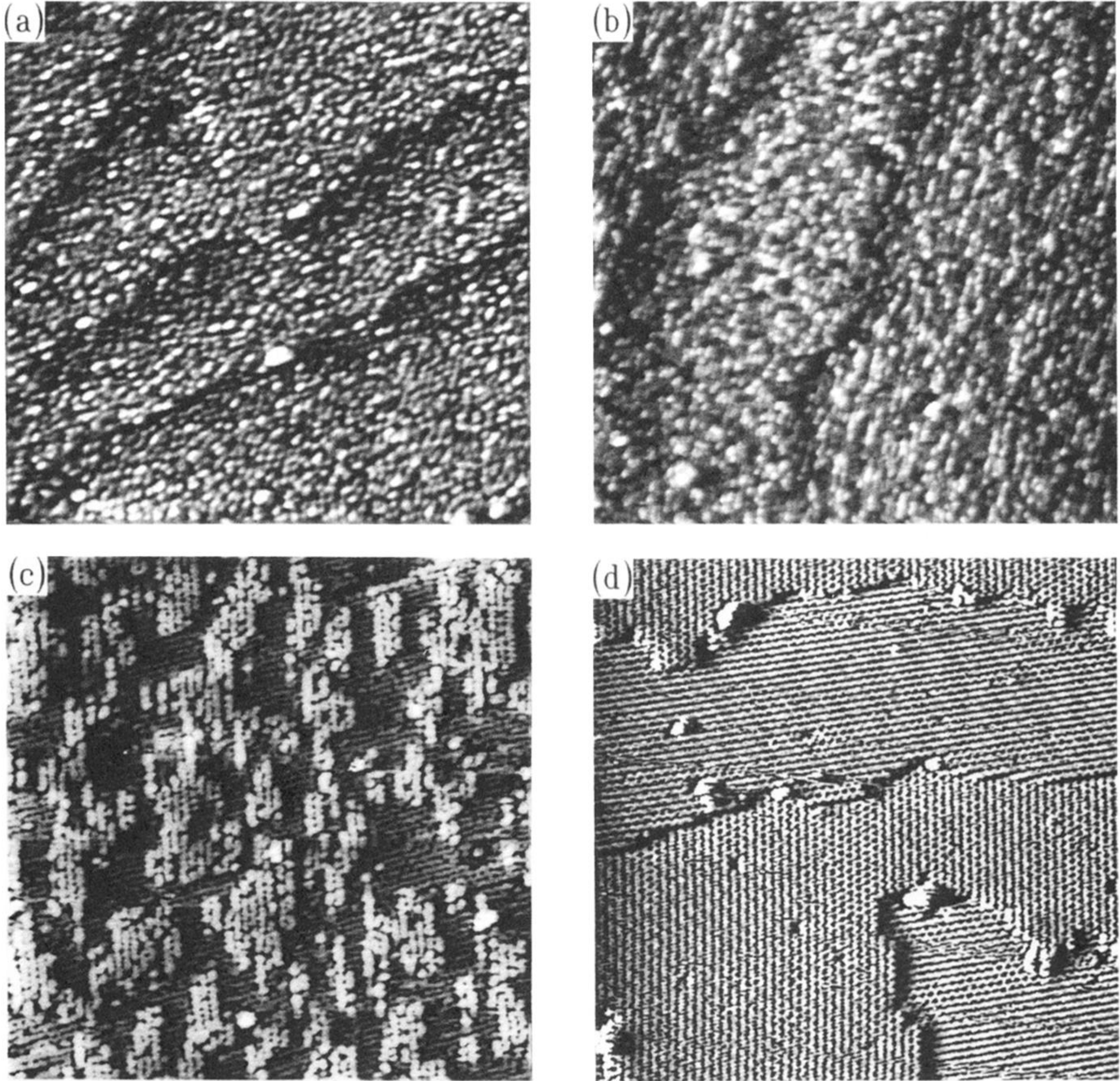

FIG. 7. STM images of (a) Ge(100)-(2×1) saturated with a 5-L disilane dose at 300 K and the same surface after annealing to (b) 530 K, (c) 620 K, and (d) 720 K. The scanned areas are 500×500 $Å^2$.